Journal of Molecular Catalysis B: Enzymatic 62 (2010) 288–296

Contents lists available at ScienceDirect

Journal of Molecular Catalysis B: Enzymatic

journal homepage: www.elsevier.com/locate/molcatb

# Disparity in productive binding mode of the slow-reacting enantiomer determines the novel catalytic behavior of *Candida antarctica* lipase B

Tao Xu, Lujia Zhang, Erzheng Su, Dongbing Cui, Xuedong Wang*, Dongzhi Wei*

*State Key Laboratory of Bioreactor Engineering, East China University of Science and Technology, Shanghai 200237, China*

ARTICLE INFO

*Article history:*
Received 12 June 2009
Received in revised form
15 November 2009
Accepted 24 November 2009
Available online 1 December 2009

*Keywords:*
*Candida antarctica* lipase B
Molecular dynamics simulation
Enantioselectivity
Productive binding mode

ABSTRACT

In the context of specifying the origin of enzyme enantioselectivity, the present study explores the lipase enantioselectivity towards secondary alcohols of similar structure from the perspective of substrate binding. By carrying out molecular mechanics minimization as well as molecular dynamics simulation on tetrahedral reaction intermediates which are used as a model of transition state, we identify an unconventional productive binding mode (PBM)—M/H permutation type for *Candida antarctica* lipase B (CALB). The in silico results also indicate that different PBMs of the slow-reacting enantiomer do exist in one lipase even when there is little structural differences between substrates, e.g. compounds with Ph or $CH_2CH_2Ph$ group display the M/H permutation type PBM while molecules with $CH_2Ph$ show the M/L permutation type PBM. By relating the PBMs of substrates to the experimentally determined *E*-values obtained by Hoff et al. [16], we find that disparity in PBM of the slow-reacting enantiomer determines why *E*-values of substrates with $CH_2Ph$ were lower than *E*-values of substrates with Ph or $CH_2CH_2Ph$ group. The modeling results also suggest that the "pushed aside" effect of the F atom and Br atom accommodates the medium size substituent of the substrate better in the stereospecificity pocket of the enzyme.



## 1. Introduction

Lipases have been widely used in academia and industry because of their high catalytic activity and stability in organic solvents as well as their broad substrate specificity and high enantioselectivity [1,2]. While biotechnologists pay increasing attentions to its application in resolution of racemic compounds [3,4], they look for the origin of its enantioselectivity as well. In early days when few crystal structures were available, only a simple "empirical rule" based on the sizes of the substituents at the stereocenter (Fig. 1) was used to predict the fast-reacting enantiomer of secondary alcohol [5]. Nowadays, due to the great progress that has been made in structure determination, plenty of crystal structures of lipases are available and have been applied to elucidate the mechanism of lipase enantioselectivity by series of elaborate modeling studies [6–10].

Most researchers attributed lipase enantioselectivity to the differences of productive binding modes between the fast-reacting enantiomer and the slow-reacting enantiomer. While they agreed on the PBM of the fast-reacting enantiomer (Fig. 2a), most modeling studies of lipase enantioselectivity towards secondary alcohols suggested that the slow-reacting enantiomer reacted via an M/L permutation [11–14] despite that other orientations were proposed (Fig. 2b) [15]. Although the possibility of other PBMs may exist, it has not yet been reported as far as our knowledge goes. Besides, the idea that orientation may differ for different secondary alcohols with a single lipase was proposed nearly a decade ago [15], it has not yet been verified because of the absence of appropriate experimental observations.

Such experimental clues, however, may exist. Hoff et al. [16] obtained an unexpected experimental result when they exploited CALB for the resolution of racemic C-3 synthons (Fig. 1 of supplementary materials 1). They found that *E*-values of the substrate with Ph or $CH_2CH_2Ph$ group were always higher than *E*-values of substrates with $CH_2Ph$ group when other conditions (e.g. $R_1$ group, acyl donor, temperature, solvent) were the same (Table 1 of supplementary materials 1). When the same acyl donor (2-chloroethyl butanoate) was used for reaction, the *E*-values of compounds 1 and 3 were much higher than compound 2.

Past modeling studies suggested that the strong *R* selectivity of CALB was caused by an M/L permutation of substrate binding [13,14]. The fast-reacting enantiomer (R-enantiomer) positioned its medium-sized substituent in the stereospecificity pocket [17] and its large substituent toward the active site entrance while the medium-sized substituent of the slow-reacting enantiomer (S-enantiomer) was pointed toward the active site entrance and its

*Abbreviations:* CALB, *Candida antarctica* lipase B; MM, molecular mechanics; MD, molecular dynamics; TI, tetrahedral intermediate; PBM, productive binding mode.

* Corresponding authors. Tel.: +86 021 64252413; fax: +86 021 64250068.
*E-mail addresses:* robertxutao@mail.ecust.edu.cn (T. Xu), ljzhang@ecust.edu.cn (L. Zhang), ezhsu@ecust.edu.cn (E. Su), xdwang@ecust.edu.cn (X. Wang), dzhwei@ecust.edu.cn (D. Wei).

1381-1177/$ – see front matter © 2009 Elsevier B.V. All rights reserved.
doi:10.1016/j.molcatb.2009.11.011

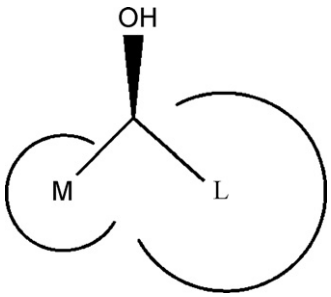


**Fig. 1.** Empirical rules to predict the fast-reacting enantiomer of secondary alcohol. L and M represent the large- and medium-sized substituents at the stereocenter of the alcohol. For esters of secondary alcohols, the enantiomer shown reacts faster with cholesterol esterase, *Pseudomonas cepacia* lipase and *Candida rugosa* lipase.

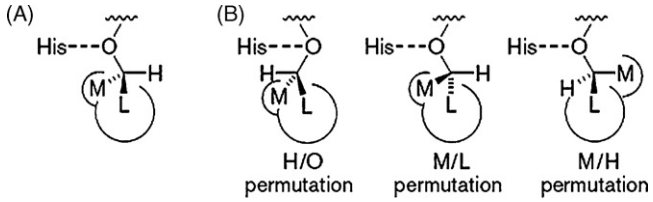


**Fig. 2.** Proposed catalytically productive orientations of secondary alcohols in the active site of lipases. (a) Researchers agree that catalytically productive orientation for the fast-reacting enantiomer has the medium and large substituents in their respective pockets and the alcohol oxygen pointing toward the catalytic histidine. (b) Several possible orientations have been proposed for the slow-reacting enantiomer, however. The figure was reproduced from Kazlauskas et al. [5].

**Table 1**
Productive binding modes of the slow-reacting enantiomer determined by molecular mechanics minimization.

| Substrate | $R_1$ | $R_2$ | PBMs of S-enantiomer |
|---|---|---|---|
| 1 | H | Ph | M/H |
| 2 | H | $CH_2Ph$ | L/M |
| 3 | H | $CH_2CH_2Ph$ | M/H |
| 4 | F | Ph | M/H |
| 5 | F | $CH_2Ph$ | L/M |
| 6 | F | $CH_2CH_2Ph$ | M/H |
| 7 | Cl | Ph | M/H |
| 8 | Cl | $CH_2Ph$ | L/M |
| 9 | Cl | $CH_2CH_2Ph$ | M/H |
| 10 | Br | Ph | M/H |
| 11 | Br | $CH_2Ph$ | L/M |
| 12 | Br | $CH_2CH_2Ph$ | M/H |

large substituent is placed in the stereospecificity pocket (Fig. 3). According to this rule, adding to or removing just one carbon atom from the large group of substrate will not greatly increase the enantioselectivity (*E*-value) of the reaction when other catalytic conditions (i.e., temperature, acyl donor) are the same. Although the kinetic reason for Hoff's observation has been identified to be a higher rate for the slow-reacting enantiomer [16], what this means on a molecular level is not yet known.

In the present study, we aim to elucidate the molecular mechanism of Hoff's observation by relating the PBM of the slow-reacting enantiomer to the experimentally determined *E*-value. Furthermore, the existence of other type of PBM as well as the idea that orientation may differ for different secondary alcohols with a single lipase will be inspected and verified.

## 2. Materials and methods

The modeling was performed using the SYBYL molecular modeling package version 7.3 (Tripos Inc.) on a SGI Octane workstation. The enzyme–substrate system was described by using Tripos force field for the purposes of energy minimization, MD simulations, and potential energy calculations when analyzing structures.

Nonbonded cutoff distance of 8 Å and a distance-dependent dielectric function with a scaling factor of one were used in all calculations. An NVT ensemble (i.e., constant number of atoms, temperature, and volume), a temperature of 300 K (aside from a short warm-up phase, see Section 2.3) and a time step of 2 fs were used in all MD simulations. All bonds connected to hydrogen atom were constrained using the shake algorithm.

### 2.1. Structural description and preparation of CALB

Crystal structure of CALB shows that its active site is buried in the core of the enzyme [18]. And the enzyme contains a catalytic triad (Ser105–His224–Asp187), an oxyanion hole (Thr40 and Gln106) that stabilizes the transition state as well as a cavity called the stereospecificity pocket [17]. The bottom of the pocket is defined by Trp104. Binding site of CALB has a funnel-like shape and during a typical reaction, an ester is bound in the acyl- and alcohol-binding sites (Fig. 4). The alcohol-binding part, which contains the stereospecificity pocket, gives CALB high substrate selectivity towards secondary alcohols [19].

The crystal structure of the free CALB enzyme (PDB code 1TCA) [19] was used as the starting point for the modeled transition state system. The substrate was built into the free enzyme rather than into the transition state analog crystal structure (PDB code 1LBS)

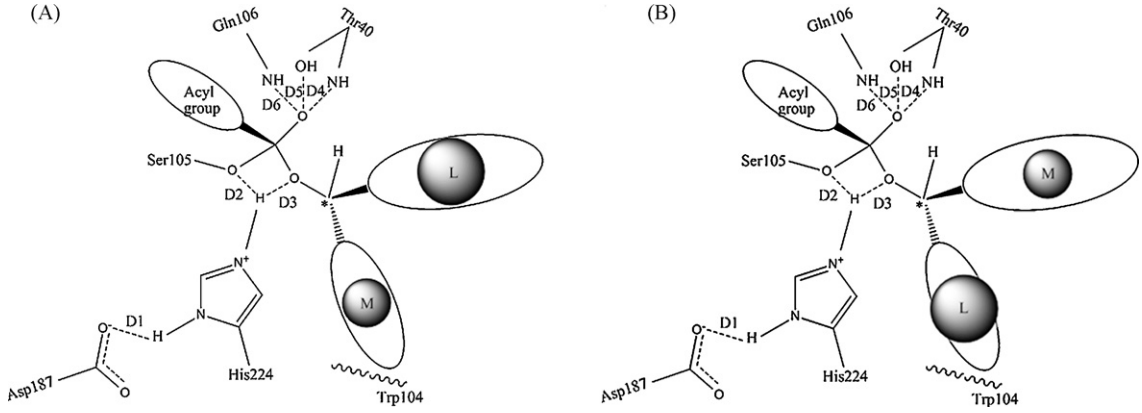


**Fig. 3.** Catalytically productive binding modes of secondary alcohols in the active site of CALB. L and M represent the large- and medium-sized substituents at the stereocenter of the alcohol. "∼∼∼∼" described the bottom of the stereospecificity pocket. The acyl part of the ligand is a butyrate group. (A) Productive binding mode of the fast-reacting enantiomer (R-enantiomer). (B) Productive binding mode of the slow-reacting enantiomer (S-enantiomer). The S-enantiomer displays an M/L permutation.

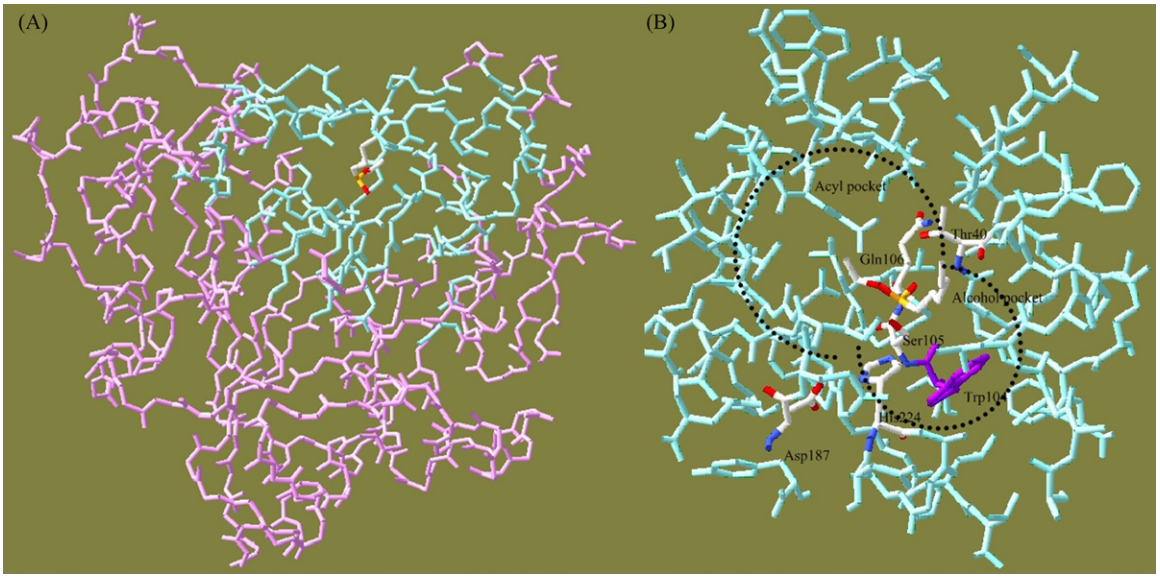


**Fig. 4.** Transition state analog crystal structure of CALB (PDB id: 1LBS) and its binding site. (A) Side-view of the structure. Only the backbone atoms were displayed. Its binding site is colored cyan. The ligand is colored by atom type. (B) Overlooking of the binding site. The residues involved in binding site include: 37–43, 46–48, 71–73, 76, 79, 103–110, 131–142, 144–145, 150–159, 161, 163–164, 183, 187–193, 201–202, 223–229, 275–288. Acyl- and alcohol-binding pockets are circled by dashed lines. Residues in the active site are colored by atom type. The bottom of the stereospecificity pocket (Trp104) is colored purple. (For interpretation of the references to color in the citation of this figure, the reader is referred to the web version of the article.)

[18] because the crystal structure of the former has been solved to a higher resolution (i.e., 1.55 Å in 1TCA compared with 2.6 Å in 1LBS). The two N-acetyl-D-glucosamine (NAG) moieties in the free CALB structure were removed. Hydrogen atoms were then added to both the enzyme and the water molecules automatically by the "Build Edit»>Add»>Hydrogen" command of SYBYL program. For adding the hydrogen atoms, SYBYL first runs "BIOPOLYMER ADD" command and then runs the "Fill valence" command. The catalytic histidine, His 224, was defined as protonated. Since the positions of many of the enzyme hydrogen atoms and all of the water hydrogen atoms were ambiguous in 1TCA, a rigorous optimization of hydrogen atom positions was performed by the method reported by Raza et al. [20].

### 2.2. Preparation of possible binding orientations of the tetrahedral intermediate system

The present MD study was based on the modeled CALB–substrate transition states of the acyl alcohol (see Fig. 2 of supplementary materials 2), which were described by the

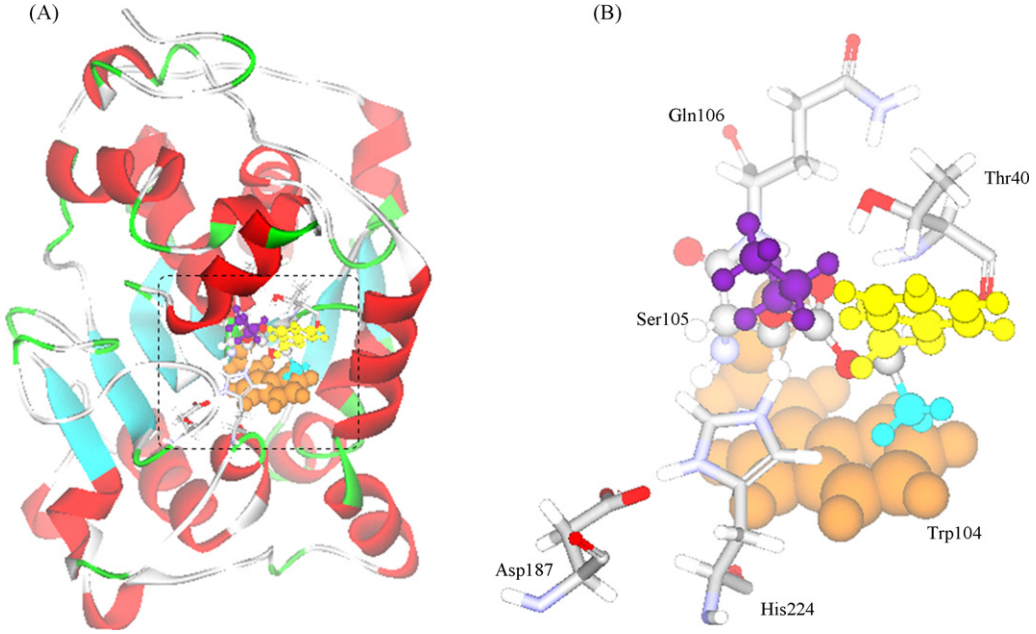


**Fig. 5.** Initially built tetrahedral intermediate of the fast-reacting enantiomer of substrate 1. (A) The panoramagram of TI. The substrate was at the active site of CALB. Region in the dash line box was enlarged in B. (B) Active site of the TI. The His224 and Asp187 of the catalytic triad, as well as the oxyanion hole (Thr40 and Gln106) were presented as stick. Ser105 and the ligand were presented as ball and stick. Trp104 which defined the bottom of the stereospecificity pocket was presented in CPK model and colored khaki. The larger group of the ligand was colored yellow, the medium size substituent was colored cyan and the acyl part of the ligand (butyrate group) was colored purple. (For interpretation of the references to color in the citation of this figure, the reader is referred to the web version of the article.)

corresponding tetrahedral intermediates. The idea that tetrahedral intermediates were used to describe the transition states of the reaction was reasonable because the free energy differences between them were very small (Fig. 3 of supplementary materials 2) [21]. Besides, Hult and his coworkers have applied the same method to study the enantioselectivity of CALB successfully [20]. So in the following part of the paper, tetrahedral intermediates were used to describe and represent the transition states of the reaction.

According to the reaction mechanism of CALB (Fig. 2 of supplementary materials 2), two transition states (TS1 and TS2) were involved. However, only TS2 would be important in the resolution of alcohols because the alcohol was not present in TS1. So in this paper, only TS2 was built and used for modeling.

The tetrahedral intermediate (TI) form of the substrate was manually modeled. The crystal structure of CALB with (1) a phosphonate inhibitor, that is, a transition state analog (PDB code 1LBS) and (2) an ester with a sufficiently long acyl chain on which to base the conformation of the acyl moieties in the models (PDB code 1LBT) [18] were used to help accommodate the acyl moiety and alcohol moiety of the substrate (Fig. 5). The alcohol moieties of all 12 substrates were modeled in both *R* and *S* configurations. For each enantiomeric configuration of the alcohol moiety, PBM of the fast-reacting enantiomer (Fig. 6A) and four different possible binding orientations (Fig. 6B–E) of the slow-reacting enantiomer proposed by Kazlauskas [15] were manually modeled for the case.

Although different acyl donors, namely 2-chloroethyl butanoate, 2,2,2-trifluoroethyl butanoate and vinyl butanoate, were used by Hoff (Table 1 of supplementary materials 1), they contained the same acyl part—a butyrate group which was necessary for building the TI. So the butyrate group was used to build the TI as the acyl moiety.

The free structure 1TCA has 286 water molecules. In our modeling structure, four water molecules ($H_2O$ 130, $H_2O$ 149, $H_2O$ 238, and $H_2O$ 285) were removed from the active site cavity to make room for the substrate. It was also noted that the six hydrogen bonds which were necessary for forming the TI2 of the reaction

**Table 2**
Productive binding modes of the slow-reacting enantiomer determined by molecular dynamics simulation.

| Substrate | $R_1$ | $R_2$ | PBMS of S-enantiomer |
|---|---|---|---|
| 1 | H | Ph | M/H |
| 2 | H | $CH_2Ph$ | L/M |
| 3 | H | $CH_2CH_2Ph$ | M/H |
| 4 | F | Ph | M/H |
| 5 | F | $CH_2Ph$ | L/M |
| 6 | F | $CH_2CH_2Ph$ | M/H |
| 7 | Cl | Ph | M/H |
| 8 | Cl | $CH_2Ph$ | L/M |
| 9 | Cl | $CH_2CH_2Ph$ | M/H |
| 10 | Br | Ph | M/H |
| 11 | Br | $CH_2Ph$ | L/M |
| 12 | Br | $CH_2CH_2Ph$ | M/H |

(Fig. 3) were kept in all of the initial binding modes during the building process (Table 2 of supplementary materials 3).

### 2.3. Molecular mechanics and dynamics

Enzyme backbone was fixed during all simulations. Atoms that were fixed were defined as an aggregate. The geometry of the aggregate was protected. And forcefield components inside it were not calculated, thus the simulation time of the TI system would be greatly reduced. However, this would not introduce an unnecessary artificial restraint to the simulation because of the rigidity of CALB. CALB has been proved to be rather rigid. A recent publication [22] studied the stability of the structure of CALB in different solvents, including water, methanol, chloroform, isopentane, toluene and cyclohexane by using molecular dynamics simulation. His results showed that the simulated structure was independent of the solvent, and had a low RMSD deviation from the crystal structure (0.4–0.8 Å) [22]. Also, the identified flexible regions showed decrease in flexibility in order of decreasing dielectric constant of the solvent (in the order methanol, isopentane, chloroform, toluene, and cyclohexane). According to the Hoff's experimen-

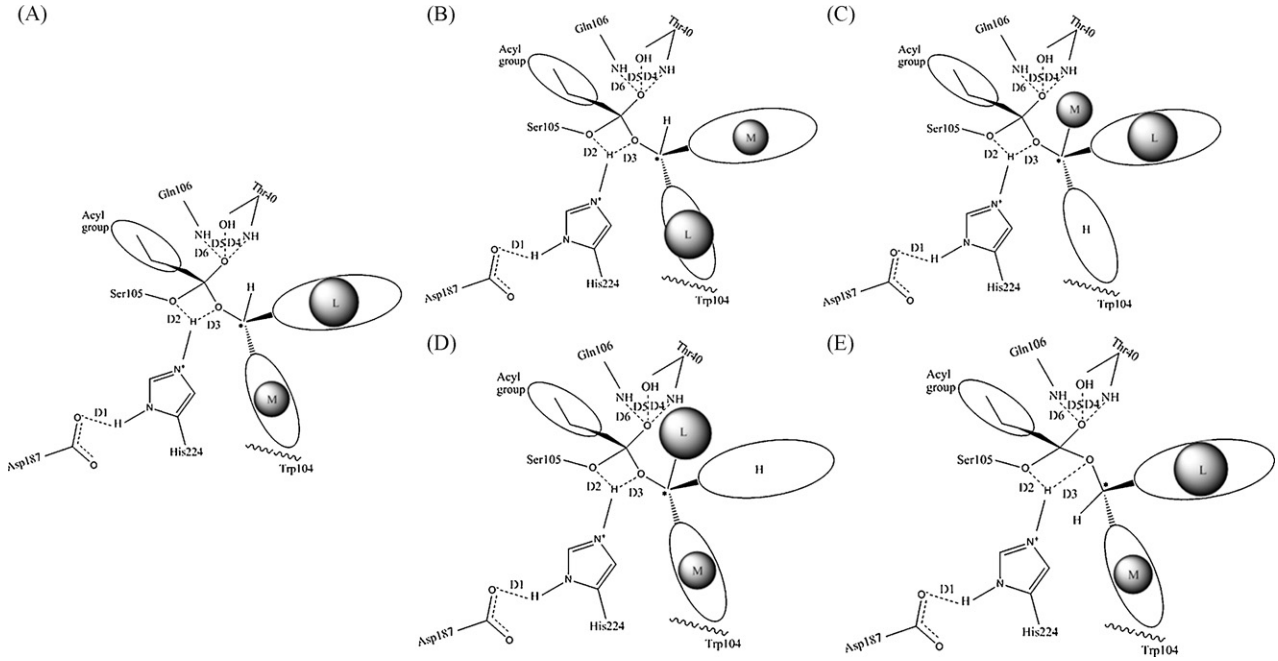


**Fig. 6.** Possible catalytically binding orientations of secondary alcohols in the active site of lipases. L and M represent the large- and medium-sized substituents at the stereocenter of the alcohol. "∼∼∼∼" described at the bottom of the stereospecificity pocket. The acyl part of the ligand is a butyrate group. (A) Productive binding modes of the R-enantiomer. (B)–(E) Displayed several possible binding orientations for the S-enantiomer. (B) An M/L permutation of binding mode. (C) An M/H permutation of binding mode. (D) An L/H permutation of binding mode and (E) An H/O permutation of binding mode.

tal procedures, substrates that were modeled in this study were solvated in hexane when the reaction was carried out [16]. This suggested that the enzyme structure was much less flexible because the dielectric constant of hexane was approximate to cyclohexane. Since the enzyme would not undergo large structural change, we could fix the backbone of the enzyme in this study.

Energy minimizations were performed by using the Powell method. Each TI ran 250 iterations of energy minimizations. However, all the H/O permutation binding modes of the S-enantiomer switched to a new conformation which looked similar to the conformation of the PBM of R-enantiomer after the minimization. So this type of binding modes was not included in further analysis. Then, each energy-minimized CALB–substrate complex ran through an MD warm-up phase to a temperature of 300 K in a series of six steps at 50 K intervals, where the simulated duration of each interval was 2 ps. The MD was carried out in a canonical ensemble (NVT). Seeing that all TIs shared nearly the same structure, they may get equilibrated at the same time period as well. So a 1-ns long MD simulation was first performed on both M/L permutation and M/H permutation binding modes of S-enantiomer of substrate 1 to evaluate the time for the TIs of reaching the equilibrium. As seen in Fig. 4 of supplementary materials 4, the TIs reached equilibrium after about 180 ps. According to this result, a 200-ps long MD simulation was performed on all TIs. A sample structure was extracted at every 0.1 ps from each simulation. Investigative analyses were performed on the last 20 ps of each simulation, yielding an ensemble of 200 nonminimized structures for each system.

### 2.4. Definition of catalytic productive binding mode

The enzyme–substrate binding conformation containing hydrogen bonds characteristic for TI (Fig. 3A): O$\delta$2 (Asp187)...H$\delta$1 (His224), H$\varepsilon$ (His224)...O$\gamma$ (Ser105), H$\varepsilon$ (His224)...O (alcohol), hydrogen bonds between oxyanion ($O^-$) and hydrogen atom connected to the backbone nitrogen of Thr40 and Gln106, hydrogen bond between oxyanion ($O^-$) and hydrogen atom of hydroxyl group of Thr40 were defined as a catalytic PBM. A broad definition of the hydrogen bond was used [23]. So a value of 3 Å cutoff was used to define its distance. For S-enantiomer, if all binding conformations met the hydrogen bond requirement, the one with the lowest energy was defined as the catalytic PBM.

## 3. Results and discussion

### 3.1. Productive binding modes of enzyme–substrate complex determined by molecular mechanics minimization

PBMs of the fast-reacting enantiomer (Table 3 of supplementary materials 5) show that no key hydrogen bonds which are required for TI are missing. However, all the H/O permutation binding modes of the S-enantiomer are not included in the analysis, because they switched to a new conformation which looked similar to the conformation of the PBM of R-enantiomer after the minimization. It is also shown that potential energies of the fast-reacting enantiomer are always lower than any binding modes of the corresponding slow-reacting enantiomer (S-enantiomer).For example, potential energy of the PBM of R-enantiomer of substrate 1 (−3854.49 kcal/mol) is lower than potential energies of all other three binding modes of S-enantiomer. This suggests that the R-enantiomer is more favored by CALB, which complies with the experimental observations of Hoff et al. [16].

As Fig. 7 suggests, binding modes of the minimized TI of substrate 1 (including the binding mode of the fast-reacting enantiomer and the M/L, M/H, L/H binding modes of the slow-reacting enantiomer) show small deviations from the corresponding initially built binding modes. The RMSD between the initially built TI and the minimized TI are not more than 0.27 Å. This indicates that no huge structural changes are introduced in the minimization step. Further more, the ligands which are allowed to move freely in TI shows an average RMSD of 0.97 Å, suggesting that the ligands are also relatively stable.

**Table 3**
Correlation between PBMs of S-enantiomer and experimentally determined *E*-value from different acyl donors.

| Substrate | $R_1$ | $R_2$ | PBMs of S-enantiomer | *E*-value | Acyl donor |
|---|---|---|---|---|---|
| 1 | H | Ph | M/H | 139 | 2-CEB |
| 2 | H | $CH_2Ph$ | L/M | 22 | 2-CEB |
| 3 | H | $CH_2CH_2Ph$ | M/H | 319 | 2-CEB |
| 4 | F | Ph | M/H | 490 | 2,2,2-TFEB |
| 5 | F | $CH_2Ph$ | L/M | 17 | 2,2,2-TFEB |
| 6 | F | $CH_2CH_2Ph$ | M/H | 375 | 2,2,2-TFEB |
| 7 | Cl | Ph | M/H | 83 | 2-CEB |
| 8 | Cl | $CH_2Ph$ | L/M | 23 | 2-CEB |
| 9 | Cl | $CH_2CH_2Ph$ | M/H | 41 | 2-CEB |
| 10 | Br | Ph | M/H | 58 | VB |
| 11 | Br | $CH_2Ph$ | L/M | 9 | VB |
| 12 | Br | $CH_2CH_2Ph$ | M/H | 52 | VB |

Acyl donor 2-CEB, 2,2,2-TFEB, VB represents the 2-chloroethyl butanoate, 2,2,2-trifluoroethyl butanoate and vinyl butanoate, respectively [16]. For the significance of $R_1$ and $R_2$, see Fig. 1 of supplementary materials 1. $1.31 \times 10^{-4}$ mol substrate and $6.55 \times 10^{-4}$ mol acyl donor were added to the hexane system (3 ml). The reaction was started by adding CALB (20 mg). Reaction temperature was 30 °C.

Situation for PBMs of the slow-reacting enantiomers is more complicated. To our great surprise, an M/H permutation is always presented as the PBM if the substrates has Ph or $CH_2CH_2Ph$ group, while the M/L permutation can only be found in compounds carrying with the $CH_2Ph$ group. This is quite different from what was found in the past study. As has been mentioned, past modeling studies of CALB suggested that the slow enantiomer always reacted via an M/L permutation. Besides the M/H permutation has been shown to mistakenly predict the fast react enantiomer of *Pseudomonas cepacia* lipase [24,25]. So we wonder whether the emergence of the M/H permutation as well as its coexistence with M/L permutation in one lipase is a new discovery or just a computation error.

Main computation error would come from the fact that MM minimization method is over-simplified by nature. According to the classic thermodynamics principles, enantioselectivity of an enzyme originates from the free energy difference between the diastereomeric transition states for reaction of the enantiomers, $\Delta\Delta G$ (Eq. (1)):

$$\ln E = -\frac{\Delta_{R-S}\Delta G}{RT} = -\frac{\Delta_{R-S}\Delta H}{RT} = \frac{\Delta_{R-S}\Delta S}{R} \quad (1)$$

Potential energy of molecular mechanics minimized complexes, however, represents only the enthalpy term ($\Delta\Delta H$). While more and more studies have proven that entropic part play an equally important role as enthalpy [26–28], MM minimization which ignores the entropic part can result in a ghastly error.

To exclude the error caused by the MM minimization, we further exploited MD simulation to the system, performed investigative analysis on ensembles of nonminimized structures from the MD simulation to reflect the inclusion of the entropic component of the system, and so related the potential energies of the system to free energies.

For our TI system, MD was carried out in a canonical ensemble system (see Section 2.3 of Section 2). The dynamics simulation performed under constant temperature and volume actually give Helmholtz free energy *F* [29]. And the relationship between Helmholz free energy *F* and enthalpy *S* is described by Eq. (2)

$$F = U - TS \quad (2)$$

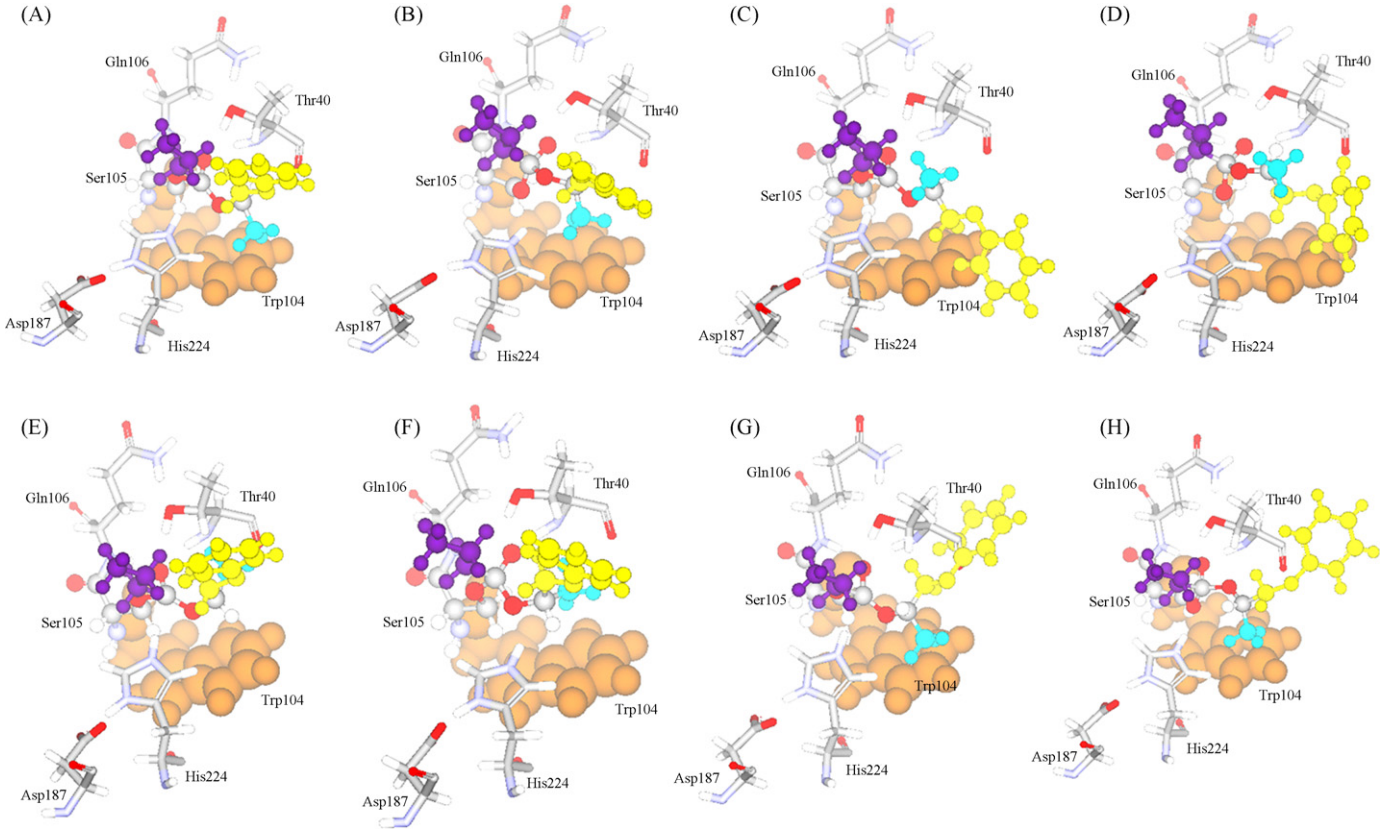


**Fig. 7.** Structural comparisons between the initially built binding modes of TI and the minimized binding modes of TI of both enantiomers of substrate 1. (A) Initially built binding mode of TI of the fast-reacting enantiomer; (B) minimized binding mode of TI of the fast-reacting enantiomer; (C) initially built M/L permutation type binding mode of the slow-reacting enantiomer; (D) minimized M/L permutation type binding mode of the slow-reacting enantiomer; (E) initially built M/H permutation type binding mode of the slow-reacting enantiomer; (F) minimized M/H permutation type binding mode of the slow-reacting enantiomer; (G) initially built L/H permutation type binding mode of the slow-reacting enantiomer and (H) minimized M/H permutation type binding mode of the slow-reacting enantiomer. The colors for displaying the figure were the same as those of Fig. 5. (For interpretation of the references to color in the citation of this figure, the reader is referred to the web version of the article.)

In this equation, $U$ stands for the internal energy of the system. The relation between $G$ and $F$ is given by $G = F + pV$ [20]. Thus, ensembles of nonminimized structures from the MD simulation in this study could reflect the inclusion of the entropic component of the system.

It is noted that the L/H permutation binding mode of S-enantiomer is not subjected to the MD simulation because of two reasons which made the binding pattern less possible to be the PBM: first, none of the twelve substrates with the L/H permutation possessed all key hydrogen bonds; second, potential energies of most L/H permutation complexes were much higher than other binding modes for the same compound.

### 3.2. Productive binding modes of enzyme–substrate complex determined by molecular dynamics simulation

For fast-reacting enantiomer, all six key hydrogen bonds required for TI exist in the PBM. And its potential energy which is expressed as the average values of the 200 nonminimized complexes, is still lower than any binding orientations of the corresponding slow enaniomer (Table 4 of supplementary materials 6) even the entropic components of the free energy are included.

For slow-reacting enantiomer, the M/H permutation is still presented as the PBM if the substrates has Ph or $CH_2CH_2Ph$ group, while the M/L permutation can be only found in compounds carrying the $CH_2Ph$ group. Although determination of the PBM of the S-enantiomer for compound 12 is blurry because of its missing necessary hydrogen bond, we still regard its M/H permutation to be a PBM because of its lower potential energy than M/L permutation.

The table also displays that average RMSD for enzyme and ligand are around 0.41 Å and 0.92 Å, respectively, this suggests that there are no tremendous structural changes for the TI structure after the MD simulation (Fig. 8).

### 3.3. Relating the PBM of slow-reacting enantiomer to the experimentally determined E-value

By relating the substrate PBMs to the experimentally determined $E$-values, we find that for comparable substrates (substrates 1–3,4–6,7–9,10–12 in Table 1 of supplementary materials 1), the ones with higher $E$-values always display the M/H permutation

**Table 4**
Correlation between PBMs of S-enantiomer and experimentally determined $E$-value using the same acyl donor (vinyl butanoate).

| Substrate | $R_1$ | $R_2$ | PBMs of S-enantiomer | $E$-value | Distance (Å) |
|---|---|---|---|---|---|
| 1 | H | Ph | M/H | 4 | 3.64 |
| 2 | H | $CH_2Ph$ | L/M | 1 | 3.43 |
| 3 | H | $CH_2CH_2Ph$ | M/H | 7 | 3.26 |
| 4 | F | Ph | M/H | 87 | 4.75 |
| 5 | F | $CH_2Ph$ | L/M | 4 | 5.21 |
| 6 | F | $CH_2CH_2Ph$ | M/H | 37 | 4.82 |
| 7 | Cl | Ph | M/H | 11 | 3.14 |
| 8 | Cl | $CH_2Ph$ | L/M | 13 | 3.17 |
| 9 | Cl | $CH_2CH_2Ph$ | M/H | 15 | 2.98 |
| 10 | Br | Ph | M/H | 58 | 5.32 |
| 11 | Br | $CH_2Ph$ | L/M | 9 | 4.9 |
| 12 | Br | $CH_2CH_2Ph$ | M/H | 52 | 4.56 |

The experimental data came from Hoff et al. [16,33].

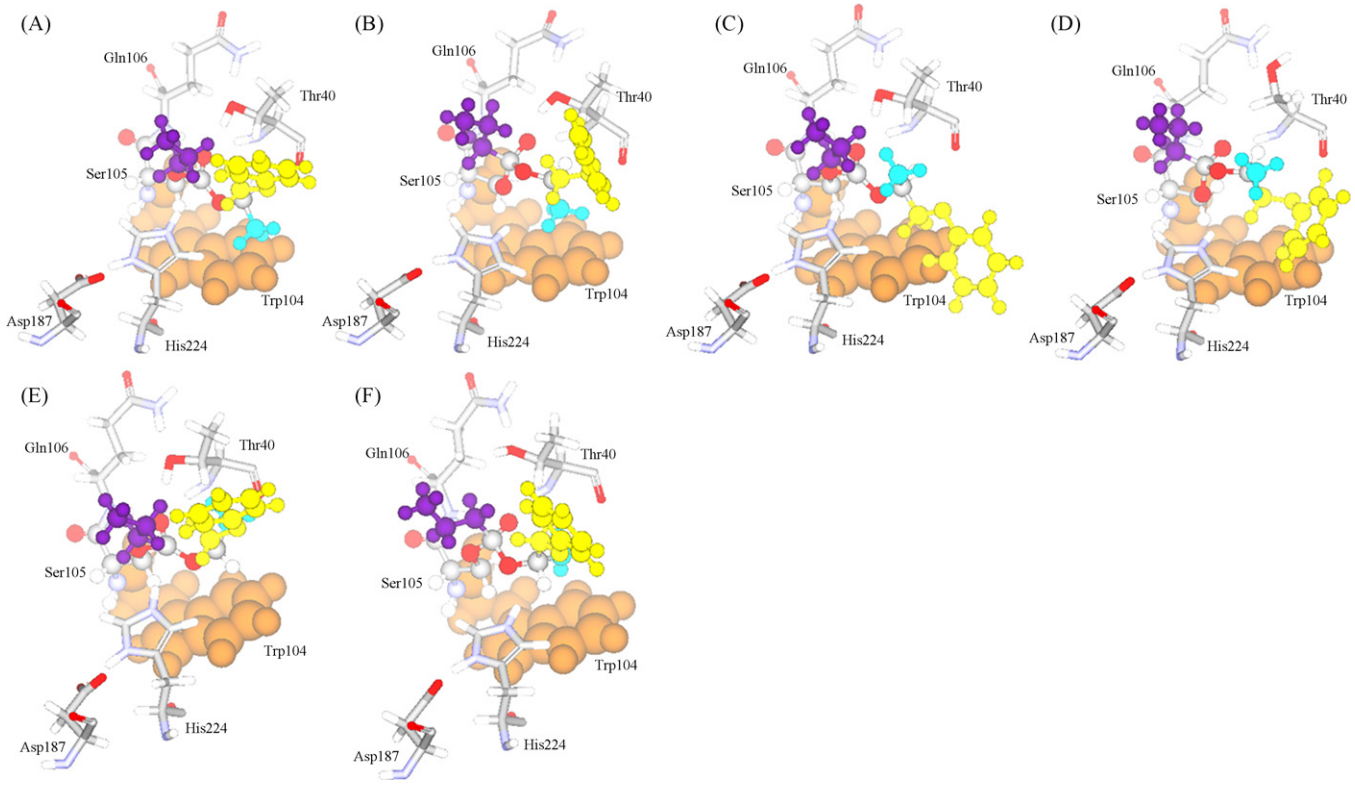


**Fig. 8.** Structural comparisons between the initially built binding modes of TI and the average TI conformation calculated from the last 200 nonminimized ensembles of the molecular dynamics simulation of substrate 1. (A) Initially built binding mode of TI of the fast-reacting enantiomer; (B) binding mode of TI of the fast-reacting enantiomer after the MD; (C) initially built M/L permutation type binding mode of the slow-reacting enantiomer; (D) M/L permutation type binding mode of the slow-reacting enantiomer after the MD; (E) initially built M/H permutation type binding mode of the slow-reacting enantiomer and (F) M/H permutation type binding mode of the slow-reacting enantiomer after the MD. The colors for displaying the figure were the same as those of Fig. 5. (For interpretation of the references to color in the citation of this figure, the reader is referred to the web version of the article.)

PBM while substrates with lower *E*-values show M/L permutation PBM (Table 3). For example, with the same acyl donor (2-chloroethyl butanoate) used, *E*-values of substrates 1 and 3 were 139 and 319, respectively. These were higher than that of substrate 2 (*E*-value of which was just 22). And the PBM of the former two compounds are found to be M/H permutation type while substrate 2 has the M/L permuation. Since the only difference between these compounds is the structure of the protecting group (compound 2 has a $CH_2Ph$ group while compounds 1 and 3 bear Ph and $CH_2CH_2Ph$ group, respectively), we come to a conclusion that disparity in productive binding mode of the slow-reacting enantiomer could cause different reaction efficiency of CALB even the structural difference between compounds is tiny.

It is noted that although different acyl donors, namely 2-chloroethyl butanoate, 2,2,2-trifluoroethyl butanoate and vinyl butanoate (see Table 1 of supplementary materials 1), were used for the resolution of the twelve racemic substrates, the same acyl donor was used for comparable substrates. For example, 2-chloroethyl butanoate was used as the acyl donor for comparable substrates 1–3, while 2,2,2-trifluoroethyl butanoate was used for comparable substrates 4–6. Thus the conclusion that disparity in PBM of the slow-reacting enantiomer could cause different reaction efficiencies of CALB has taken the effect of the acyl donors into considerations.

Even if the same acyl donor (vinyl butanoate) was used to react with all the twelve substrates, the conclusion still holds true most of the time. As Table 4 shows, for most of comparable substrates, namely substrates 1–3, 4–6, 10–12, substrates with higher *E*-values always display the M/H permutation type PBM of the slow-reacting enantiomer. The only exception exists in comparable substrates 7 and 8. Substrate 7 which possesses the M/H permutation PBM shows a lower *E*-value than substrate 8 which displays the M/L permutation PBM. This inaccuracy may come from the experimental aspect, because the difference between *E*-values of 11 and 13 could be sometimes too small to be detected using the very old gas chromatography instrument.

In conclusion, the above result provides direct evidence for Kazlauskas's prediction—productive binding orientation of different secondary alcohols can exist within a single lipase. Although the computational level of enzyme enantioselectivity has been brought up to QM or QM/MM level [30,31] due to the development of QM methodology and the advent of more powerful computers, our MD level simulations call attention to all researchers that thorough considerations of substrate binding should be achieved before further precise computational tools are used.

### 3.4. Effect of the halogens on E-values

Researchers have shown that substrates containing bromine and chlorine had a lower tendency of placing the halogen in the sterospecificity pocket [32], thus leading to lower *E*-values when they locate in the medium size substituent. And Hoff and coworkers found the same *E*-value change in their work. They attributed the change to atom polarity and size on the observation that smaller atom with fewer available electrons (H and F) gave higher *E*-value than the larger more polarizable atoms Cl and Br (Table 1 of supplementary materials 1). Their explanations, however, are ambiguous, because acyl donors which may greatly influence the *E*-value of the reaction were different in their result [33]. In fact, when the same acyl donor (vinyl butanoate) are used for all 12 substrates (Table 4), substrates with H atom and Cl atom displays much lower average *E*-value than substrates with F atom

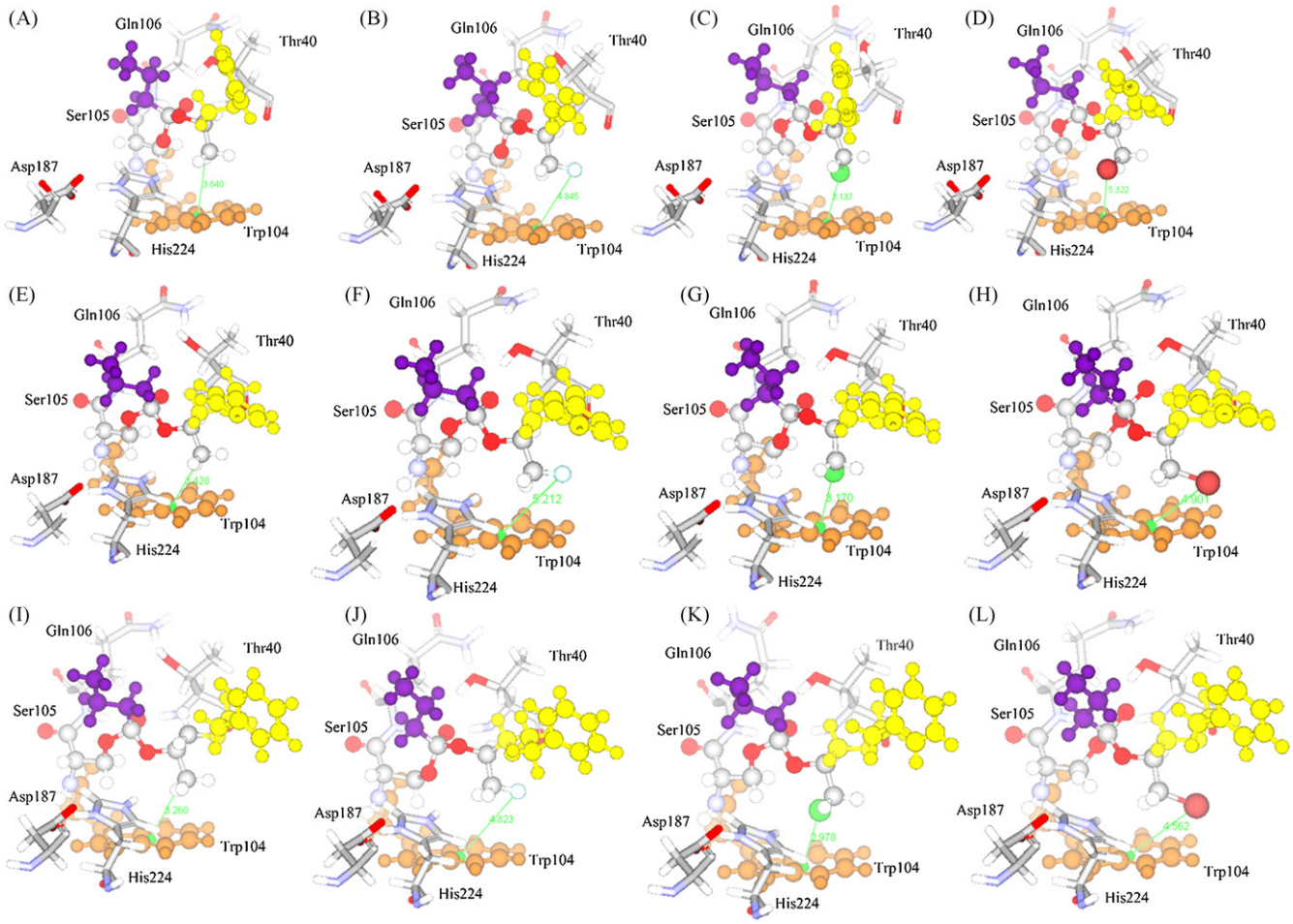


**Fig. 9.** Distances between halogen atom (or corresponding hydrogen atom) and the centroid of indole ring of Trp104. The distances were calculated from the average TI conformation of the last 200 nonminimized ensembles of the molecular dynamics simulation of the fast-reacting enantiomer of all 12 substrates. (A)–(L) were the binding mode of TI of the fast-reacting enantiomer of substrates 1–12, respectively. The colors for displaying the figure were the same as those of Fig. 5. (For interpretation of the references to color in the citation of this figure, the reader is referred to the web version of the article.)

and Br atom. In this sense, size effect and polarity effect of halogen atoms on *E*-values observed by Hoff does not hold true any more.

To further check the effect of halogen atoms size on the *E*-value, we measure the distances between $R_1$ atom of the substrate and the centroid of indole ring of Trp104 (Fig. 9), and use this distance to account for the effect of halogen atoms size on the *E*-value. This distance is crucial and sufficient for accounting for the halogen atoms size, because it could directly check the matching degree of the halogen atom of the medium size substituent to the sterospecificity pocket whose bottom was defined by Trp104.

As shows in Table 4, distances for substrates with F and Br atoms are larger than substrates with H and Cl atoms on average. And Fig. 9 suggests that the F atom and Br atom in the medium size substituent of the substrates are always "pushed aside" from Trp104 (the bottom of the sterospecificity pocket). This accommodated the medium size substituent of the substrate better in the stereospecificity pocket. Thus the reason why substrates with F atom and Br atom displayed higher *E*-values could be the "pushed aside" effect of the halogens.

## 4. Conclusions

- A new M/H permutation has been found while the conventional M/L permutation still holds true.
- Different PBMs of slow-reacting enantiomers could exist for the same selective enzyme even there is little structural differences between substrates, e.g. compounds with Ph or $CH_2CH_2Ph$ group displayed different PBMs than molecules with $CH_2Ph$.
- Disparity in productive binding mode of the slow-reacting enantiomer explains why substrates with one atom difference displayed distinct efficiency for CALB.
- The "pushed aside" effect of the F atom and Br atom made the medium size substituent of the substrate accommodate better in the stereospecificity pocket of the enzyme, and would be the reason why substrates with F atom and Br atom displayed higher *E*-values.

## Acknowledgments

The research is founded by National Basic Research Program of China (973 Program) 2009CB724703. We are grateful for anonymous reviewers for their helpful advice.

## Appendix A. Supplementary data

Supplementary data associated with this article can be found, in the online version, at doi:10.1016/j.molcatb.2009.11.011.

## References


[1] K.E. Jaeger, B.W. Dijkstra, M.T. Reetz, Annu. Rev. Microbiol. 53 (1999) 315–351.
[2] F. Hasan, A.A. Shah, A. Hameed, Enzyme Microb. Technol. 39 (2006) 235–251.
[3] C.Y. Li, P. Wang, D.T. Zhao, Y.M. Cheng, L. Wang, J. Mol. Catal. B: Enzyme 55 (2009) 152–156.
[4] Y.H. Wang, R. Wang, Q.S. Li, Z.M. Zhang, Y. Feng, J. Mol. Catal. B: Enzyme 56 (2009) 142–145.
[5] R.J. Kazlauskas, A.N.E. Weissfloch, A.T. Rappaport, L.A. Cuccia, J. Org. Chem. 56 (1991) 2656–2665.
[6] D. Guieysse, C. Salagnadb, P. Monsana, M. Remaud, Tetrahedron: Asymmetry 14 (2004) 1807–1817.
[7] S. Tomić, M. Ramek, J. Mol. Catal. B: Enzyme 38 (2006) 139–147.
[8] T. Schulz, J. Pleiss, R.D. Schmid, Protein Sci. 9 (2000) 1053–1062.
[9] B.Y. Hwang, H. Scheib, J. Pleiss, B.G. Kim, R.D. Schmid, J. Mol. Catal. B: Enzyme 10 (2000) 223–231.
[10] M. Holmquist, F. Hæffner, T. Norin, K. Hult, Protein Sci. 5 (1995) 83–88.
[11] J. Zuegg, H. Hönig, J.D. Schrag, M. Cygler, J. Mol. Catal. B: Enzyme 3 (1997) 83–98.
[12] C. Orrenius, F. Hæffner, D. Rotticci, N. Ohrner, T. Norin, K. Hult, Biocatal. Biotransform. 16 (1998) 1–15.
[13] D. Rotticci, F. Haeffner, C. Orrenius, T. Norin, K. Hult, J. Mol. Catal. B: Enzyme 5 (1998) 267–272.
[14] F. Haeffner, T. Norin, K. Hult, Biophys. J. 74 (1998) 1251–1262.
[15] R.J. Kazlauskas, Curr. Opin. Chem. Biol. 4 (2000) 81–88.
[16] B.H. Hoff, L. Ljones, A. Ronstad, T. Anthonsen, J. Mol. Catal. B: Enzyme 8 (2000) 51–60.
[17] A.O. Magnusson, J.C. Rotticci-Mulder, A. Santagostino, K. Hult, Chembiochem 6 (2005) 1051–1056.
[18] J. Uppenberg, M.T. Hansen, S. Patkar, T.A. Jones, Structure 2 (1994) 293–308.
[19] J. Uppenberg, N. Ohrner, M. Norin, K. Hult, G.J. Kleywegt, S. Patkar, V. Waagen, T. Anthonsen, T.A. Jones, Biochemistry 34 (1995) 16838–16851.
[20] S. Raza, L. Fransson, K. Hult, Protein Sci. 10 (2001) 329–338.
[21] C.H. Hu, T. Brinck, K. Hult, J. Quantum Chem. 69 (1998) 89–103.
[22] P. Trodler, J. Pleiss, BMC Struct. Biol. 8 (2008) 9–19.
[23] R.D. Gautam, S. Thomas, The Weak Hydrogen Bond: In Structural Chemistry and Biology, Oxford Science Publications, Oxford, 2001.
[24] K. Nakamura, M. Kawasaki, A. Ohno, Bull. Chem. Soc. Jpn. 67 (1994) 3053–3056.
[25] K. Nakamura, M. Kawasaki, A. Ohno, Bull. Chem. Soc. Jpn. 69 (1996) 1079–1085.
[26] P.L.A. Overbeeke, J. Ottosson, K. Hult, J.A. Jongejan, J.A. Duine, Biocatal. Biotransform. 17 (1999) 61–79.
[27] J. Ottosson, J.C. Rotticci-Mulder, D. Rotticci, K. Hult, Protein Sci. 10 (2001) 1769–1774.
[28] P.L.A. Overbeeke, S.C. Orrenius, J.A. Jongejan, J.A. Duine, Chem. Phys. Lipids 1 (1998) 81–93.
[29] R.P. White, H. Meirovitch, Proc. Natl. Acad. Sci. 101 (2004) 9235–9240.
[30] M. Luić, Z. Stefanić, I. Ceilinger, M. Hodoscek, D. Janezic, T. Lenac, I.L. Asler, D. Sepac, S. Tomić, J. Phys. Chem. B 112 (2008) 4876–4883.
[31] M. Toşa, S. Pilbákb, P. Moldovana, C. Paizsa, G. Szatzkerb, G. Szakácsc, L. Novákb, F.D. Irimiea, Tetrahedron: Asymmetry 19 (2008) 1844–1852.
[32] D. Rotticci, C. Orrenius, K. Hult, T. Norin, Tetrahedron: Asymmetry 8 (1997) 359–362.
[33] B.H. Hoff, H.W. Anthonsen, T. Anthonsen, Tetrahedron: Asymmetry 7 (1996) 3187–3192.